Spin and density excitations in the triangular-lattice *t-J* model with multiple-spin exchange interactions: ^{3}He on graphite

K. Seki,[1] T. Shirakawa,[1,2] and Y. Ohta[1]
[1]*Department of Physics, Chiba University, Chiba 263-8522, Japan*
[2]*Institut für Theoretische Physik, Leibniz Universität Hannover, D-30167 Hannover, Germany*
(Received 13 October 2008; revised manuscript received 26 December 2008; published 26 January 2009)

Using an exact-diagonalization technique on small clusters, we study spin and density excitations of the triangular-lattice *t-J* model with multiple-spin exchange interactions, whereby we consider anomalous properties observed in the doped Mott region of the two-dimensional liquid ^{3}He adsorbed on a graphite surface. We find that the double-peak structure consistent with experiment appears in the calculated temperature dependence of the specific heat; the low-temperature sharp peak comes from the spin excitations reflecting the frustrated nature of the spin degrees of freedom and high-temperature broad peak comes from the density excitations extending over the entire bandwidth. The clear separation in their energy scales is evident in the calculated spin and density excitation spectra. The calculated single-particle excitation spectra suggest the presence of fermionic quasiparticles dressed by the spin excitations, with an enhanced effective mass consistent with experiment.

DOI: 10.1103/PhysRevB.79.024303 PACS number(s): 67.30.hr, 67.80.dm

I. INTRODUCTION

^{3}He atoms adsorbed on a graphite surface are known to be an ideal two-dimensional-correlated spin-1/2 fermion system. A solidified commensurate phase of ^{3}He atoms is stabilized at a 4/7 density of the underlying layer of ^{4}He atoms due to the substrate potential corrugation and thus a triangular lattice of ^{3}He atoms is formed, which is a realization of a gapless quantum spin liquid (QSL).[1] Theoretically, this 4/7 phase of spin-1/2 ^{3}He atoms has been studied by using the triangular-lattice Heisenberg model with the multiple-spin exchange interactions.[2–7] Importance of the density fluctuations has recently been pointed out as well.[8]

A finite amount of vacancies of ^{3}He atoms can be introduced into this 4/7 phase in a stable manner, where the vacancies can hop from site to site of the triangular lattice via quantum-mechanical tunneling motions even at absolute zero temperature. The presence of such vacancies called the zero-point vacancies (ZPVs) was predicted a few decades ago.[9,10] Quite recently, the experimental evidence for the ZPVs has been reported in the monolayer of ^{3}He adsorbed on a surface of graphite preplated by a solid monolayer of ^{4}He (Refs. 11 and 12): i.e., heat-capacity measurements of the system show an anomalous coexistence of a magnetic round peak near 1 mK and a broad peak at several tens of millikelvins that are associated with the ZPVs doped into the commensurate Mott-localized solid. The ZPVs are maintained up to the doping of almost 20% of the lattice sites, which we call the doped Mott region of monolayer ^{3}He.

Theoretically, Fuseya and Ogata[13] proposed the triangular-lattice *t-J* model with four-spin ring-exchange interactions as an effective model for the doped Mott region of the system and obtained its ground-state phase diagram. The low-energy excitations of the model were also discussed. They have thereby argued that there is a new-type anomalous quantum-liquid phase characteristic of the "spin-charge separation," which may be relevant with the anomalous features observed in the doped Mott region of the monolayer ^{3}He adsorbed on a graphite surface.

Motivated by such developments in the field, we study in this paper the triangular-lattice *t-J* model with the multiple-spin exchange interactions further. In particular, we directly calculate the spin and density excitation spectra and single-particle spectra as well as the temperature dependence of the specific heat and uniform magnetic susceptibility by using an exact-diagonalization technique on small clusters. We thereby consider the anomalous properties observed in the doped Mott region of the two-dimensional liquid ^{3}He adsorbed on a graphite surface.

We will thus demonstrate that the double-peak structure actually appears in the temperature dependence of the specific heat, which is qualitatively consistent with experiment; the low-temperature sharp peak comes from the spin excitations and high-temperature broad peak comes from the density excitations. The spectral weight for the calculated spin excitation spectra is concentrated on a very low-energy region that scales with the exchange interactions, while that of the density excitations extends over an entire bandwidth that scales with the hopping parameter of the vacancy. The clear separation between spin and density excitations in their energy scales is thus found. The accumulation of the low-energy spectral weight of the spin excitations comes from the frustrated nature of the spin degrees of freedom of the system; i.e., the ferromagnetic two-spin interactions compete with the antiferromagnetic four-spin interactions on the geometrically frustrated triangular lattice. The single-particle excitation spectra suggest that the vacancies behave like fermionic quasiparticles dressed by the spin excitations, with the enhanced effective-mass consistent with experiment. Preliminary results of our work have been presented in Ref. 14.

This paper is organized as follows. In Sec. II, we present our model and method of calculation. In Sec. III, we present our results of calculations for the specific heat, magnetic susceptibility, spin and density excitation spectra, and single-particle excitation spectra. We compare our results with experiment in Sec. IV. We summarize our work in Sec. V.

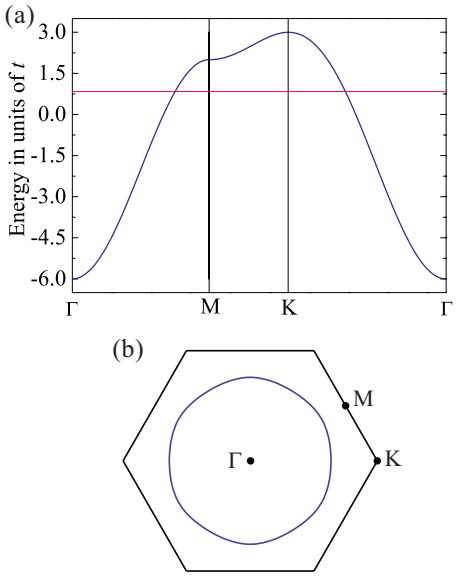

FIG. 1. (Color online) (a) Noninteracting tight-binding band structure of the triangular lattice with the nearest-neighbor hopping parameter t. Horizontal line represents the Fermi energy at half filling. (b) Brillouin zone and Fermi surface at half filling.

II. MODEL AND METHOD

The triangular-lattice t-J model with the multiple-spin exchange interactions is defined by the Hamiltonian,

$$\mathcal{H} = -t\sum_{\langle ij\rangle,\sigma}(\tilde{c}^{\dagger}_{i\sigma}\tilde{c}_{j\sigma} + \text{H.c.}) + J\sum_{\langle ij\rangle}\left(\mathbf{S}_i\cdot\mathbf{S}_j - \frac{n_i n_j}{4}\right) + K\sum_{\langle ijkl\rangle}(P_4 + P_4^{-1}) + R\sum_{\langle ijklmn\rangle}(P_6 + P_6^{-1}), \quad (1)$$

where $\tilde{c}_{i\sigma}=c_{i\sigma}(1-n_{i,-\sigma})$ is the projected annihilation operator of a fermion (^{3}He atom) at site i and spin σ ($=\uparrow,\downarrow$) allowing no doubly occupied sites, $\mathbf{S}_i$ is the spin-1/2 operator, and n_i ($=n_{i\uparrow}+n_{i\downarrow}$) is the number operator. The summation in the t-J part of the model is taken over all the nearest-neighbor pairs $\langle ij\rangle$ on the triangular lattice. P_4 and P_6 are the four-spin and six-spin exchange operators defined as $P_4=P_{il}P_{ik}P_{ij}$ and $P_6=P_{in}P_{im}P_{il}P_{ik}P_{ij}$, respectively, where $P_{ij}=(1+\boldsymbol{\sigma}_i\cdot\boldsymbol{\sigma}_j)/2$ with the Pauli-spin matrix $\boldsymbol{\sigma}_i$. The summation is taken over all the possible combinations of four nearest-neighbor sites $\langle ijkl\rangle$ for P_4 and over all the equilateral hexagons $\langle ijklmn\rangle$ for P_6, where one should note that the terms—unless all the sites are occupied by the fermion—are excluded from the summation.

In this paper, we study the dynamical properties of the model under the introduction of vacancies in the 4/7 commensurate solid phase of ^{3}He, i.e., removal of particles (^{3}He atoms) or addition of ZPVs. We thus define the filling n of particles as $n=N/L$, where N is the total number of particles and L is the total number of lattice sites in the system; in particular, $n=1$ is referred to as "half filling," which corresponds to the 4/7 solid phase. The noninteracting band structure and Fermi surface at half filling of the tight-binding model with the nearest-neighbor hopping parameter t are shown in Fig. 1; we find no nesting features in the Fermi surface and no singularities in the density of states for $n<1$.

The nearest-neighbor hopping parameter t and two-spin and four-spin exchange interaction parameters J and K have been estimated as follows:[13] $t\simeq 50-100$ mK, $-J\simeq 1-10$ mK, and $K/|J|\sim 0.2$. We note that in this parameter region, the two-spin exchange term favors the ferromagnetic spin polarization ($J<0$) but the four-spin exchange term gives the antiferromagnetic spin correlations between neighboring spins, and thus we have the situation where the strong frustration in the spin degrees of freedom of the system appears. Geometrical frustration also appears on the triangular lattice when the interaction between spins is antiferromagnetic. We have examined the effects of the six-spin exchange interaction term on the ground state and excitation spectra and found that the effects are very small, in particular, when the system is doped with vacancies. This is because the P_6 exchange interaction is easily cut by the presence of vacancies. We will therefore present the results at $R=0$ in this paper, the model of which we will hereafter refer to as the t-J-K model. Throughout the paper, we use $t=1$ as the unit of energy unless otherwise stated and we set $\hbar=k_B=1$.

We use the Lanczos exact-diagonalization technique on small clusters to calculate the ground state and excitation spectra of the model. In particular, we calculate the dynamical spin- and density-correlation functions defined, respectively, as

$$S(\mathbf{q},\omega) = -\frac{1}{\pi}\mathfrak{I}\langle\Psi_0|S^{z\dagger}_{\mathbf{q}}\frac{1}{\omega+i\eta-(\mathcal{H}-E_0)}S^{z}_{\mathbf{q}}|\Psi_0\rangle \quad (2)$$

and

$$N(\mathbf{q},\omega) = -\frac{1}{\pi}\mathfrak{I}\langle\Psi_0|n^{\dagger}_{\mathbf{q}}\frac{1}{\omega+i\eta-(\mathcal{H}-E_0)}n_{\mathbf{q}}|\Psi_0\rangle, \quad (3)$$

where Ψ_0 and E_0 are the ground-state wave function and energy, respectively. $S^z_{\mathbf{q}}$ and $n_{\mathbf{q}}$ are the Fourier transforms of the spin and particle-number operators defined, respectively, as

$$S^z_{\mathbf{q}} = \frac{1}{\sqrt{L}}\sum_i e^{i\mathbf{q}\cdot\mathbf{r}_i}S^z_i, \quad (4)$$

$$n_{\mathbf{q}} = \frac{1}{\sqrt{L}}\sum_i e^{i\mathbf{q}\cdot\mathbf{r}_i}n_i, \quad (5)$$

where $\mathbf{r}_i$ is the position of the lattice site i.

We also calculate the single-particle excitation spectrum defined as

$$A(\mathbf{q},\omega) = A^{-}(\mathbf{q},-\omega) + A^{+}(\mathbf{q},\omega), \quad (6)$$

with the particle removal spectrum

$$A^{-}(\mathbf{q},\omega) = -\frac{1}{\pi}\mathfrak{I}\langle\Psi_0|\tilde{c}^{\dagger}_{\mathbf{q}\sigma}\frac{1}{\omega+i\eta-(\mathcal{H}-E_0)}\tilde{c}_{\mathbf{q}\sigma}|\Psi_0\rangle \quad (7)$$

and particle addition spectrum

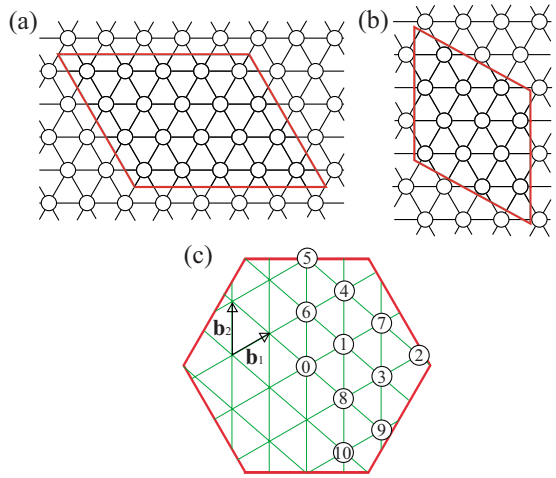

FIG. 2. (Color online) (a) 20-site and (b) 12-site clusters used for calculations. (c) Brillouin zone and available momenta of the 20-site cluster in the periodic boundary condition.

$$A^+(\mathbf{q},\omega) = -\frac{1}{\pi}\Im\langle\Psi_0|\tilde{c}_{\mathbf{q}\sigma}\frac{1}{\omega + i\eta - (\mathcal{H} - E_0)}\tilde{c}^\dagger_{\mathbf{q}\sigma}|\Psi_0\rangle, \quad (8)$$

where $\eta \to +0$, which is replaced by a small positive number in the actual calculations to give an artificial broadening of the spectra. We use a cluster of 20 sites with periodic boundary condition for these calculations (see Fig. 2), where the independent available momenta in the Brillouin zone $\mathbf{q}_0, \ldots, \mathbf{q}_{10}$ are also shown. They are at $\mathbf{q}_i = m\mathbf{b}_1 + n\mathbf{b}_2$ with $\mathbf{b}_1 = 2\pi/5(1, 1/\sqrt{3})$ and $\mathbf{b}_2 = (0, \pi/\sqrt{3})$, where (m,n) are (0,0) for $\mathbf{q}_0$, (1,0) for $\mathbf{q}_1$, (3,−1) for $\mathbf{q}_2$, (2,−1) for $\mathbf{q}_3$, (1,1) for $\mathbf{q}_4$, (0,2) for $\mathbf{q}_5$, (0,1) for $\mathbf{q}_6$, (2,0) for $\mathbf{q}_7$, (1,−1) for $\mathbf{q}_8$, (2,−2) for $\mathbf{q}_9$, and (1,−2) for $\mathbf{q}_{10}$. In the following, we will in particular examine the cluster with two vacancies, i.e., $n = 0.9$.

To calculate the temperature T dependence of the specific heat $C(T)$, magnetization $M(T)$ under uniform magnetic field h, and uniform magnetic susceptibility $\chi(T) = \lim_{h\to 0}(\partial M/\partial h)_T$, the Hamiltonian for a smaller-size cluster of 12 sites (see Fig. 2) is fully diagonalized to calculate the partition function.[15,16] We add the Zeeman term $-h\Sigma_i S_i^z$ to the Hamiltonian (1) when we calculate the magnetic response of the system. In the following, we will in particular examine this cluster with one vacancy ($n=0.92$) and two vacancies ($n=0.83$).

III. RESULTS OF CALCULATION

A. Ground-state phase diagram

The ground-state phase diagram in the parameter space of the present model at $R=0$ was obtained by Fuseya and Ogata,[13] which we have also reproduced successfully. Here, we briefly review their results. The phases obtained are as follows: the region of phase separation (phase I), the region of Fermi liquid with strong spin fluctuations (phase II), the region of new-type anomalous quantum liquid (phase III), and the region of ferromagnetism (phase IV), where we follow their notations of the phases. They have put special emphasis on the phase III, which has been argued to be the region of "spin-charge separation" and may be relevant with the anomalous features of the doped Mott region of the ^{3}He monolayer.

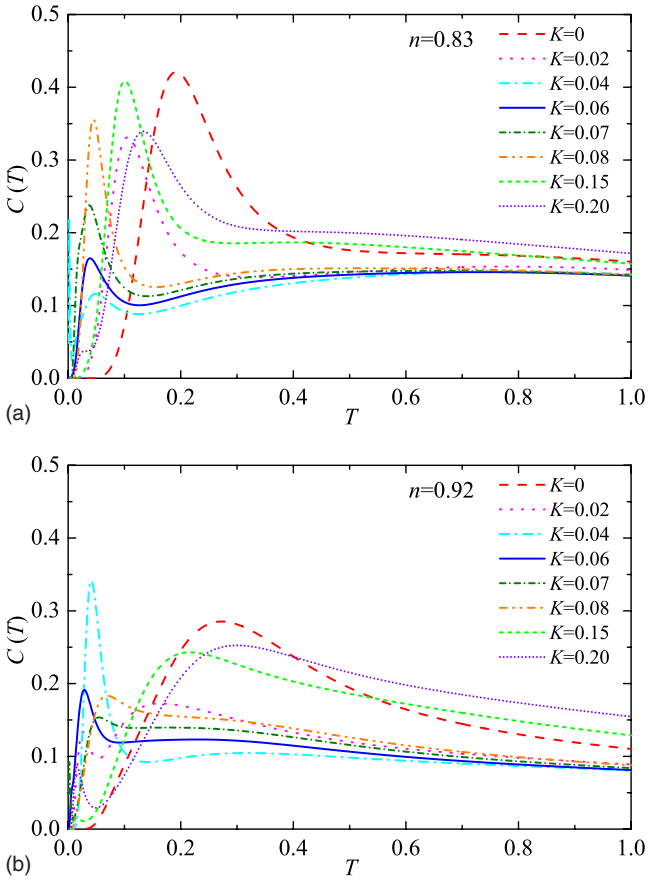

FIG. 3. (Color online) Calculated temperature dependence of the specific heat (per site) of the t-J-K model at $J=-0.3$. We use the cluster of 12 sites with two vacancies ($n=0.83$) in the upper panel and with one vacancy ($n=0.92$) in the lower panel.

In the following, we in particular examine the region of this new-type anomalous quantum liquid (phase III) using the parameter values $J=-0.3$ and $K=0.06$, which we compare with the results of other regions when necessary, i.e., the region of ferromagnetism (phase IV) using $J=-0.3$ and $K=0$ and the region of Fermi liquid (phase II) using $J=-0.3$ and $K=0.15-0.2$.

B. Specific heat and entropy

The calculated results for the temperature dependence of the specific heat $C(T)$ at $n=0.83$ and 0.92 are shown in Fig. 3. We find that there appears a double-peak structure in $C(T)$ at $K=0.06$ (corresponding to the new-type anomalous quantum-liquid phase), i.e., a sharp peak at low temperatures and a very broad peak extending over high temperatures. The double-peak structure is not clearly seen at $K=0$ and 0.15–0.2. We should note here that the specific-heat coefficient γ, where $C(T) = \gamma T$ at low temperatures, cannot be deduced from the present calculations since $C(T)$ decays exponen-

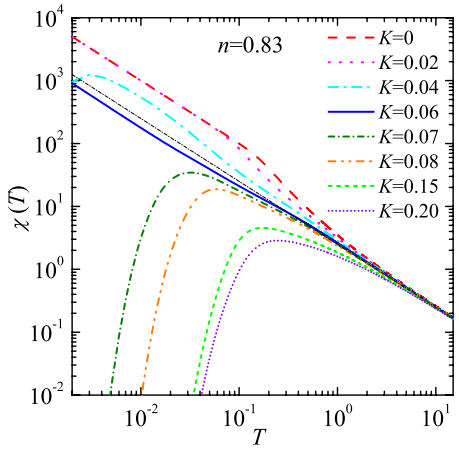

FIG. 4. (Color online) Calculated temperature dependence of the uniform magnetic susceptibility of the t-J-K model at $J=-0.3$. We use the cluster of 12 sites with two vacancies: $n=0.83$. Straight line corresponds to the Curie law $\chi(T)=C/T$, where C is the Curie constant.

tially at low temperatures due to the discreteness of the energies of finite-size systems.

We will show in Sec. III D that the low-temperature sharp peak comes from the excitation of the spin degrees of freedom of the system and the broad high-temperature peak comes from the excitations of the density degrees of freedom of the system. In other words, the width of the sharp low-energy peak scales with the exchange interactions between spins (a combination of J and K) and the width of the broad high-energy peak scales with the hopping parameter t of the vacancy.

It is interesting to note that the double-peak structure in the specific heat $C(T)$ due to the separation in their energy scales between spin and density degrees of freedom has previously been discussed in the context of the low-energy excitations in the Hubbard ladder systems with charge ordering instability, although the latter is for the insulating systems with a charge gap.[17] In Sec. IV, we will compare the obtained double-peak structure with experiment.[11,12] We also calculate the temperature dependence of the entropy $S(T)$ (not shown here), which will be compared with experiment[12] also in Sec. IV.

C. Uniform magnetic susceptibility

The calculated results for the temperature dependence of the uniform magnetic susceptibility $\chi(T)$ are shown in Fig. 4. We find that the temperature variation is strongly dependent in the value of K. (i) When $0 \leq K \lesssim 0.04$, $\chi(T)$ is strongly enhanced in comparison with the Curie susceptibility $\chi(T)=C/T$, resulting in the ferromagnetic spin polarization at low temperatures. (ii) When $K=0.06$ at which the frustration in the spin degrees of freedom is the largest, $\chi(T)$ is slightly suppressed in comparison with the Curie law. Here, the ground state is highly degenerate due to the frustration of the spin degrees of freedom; in our cluster, the degeneracy is 15-fold. (iii) When $K \gtrsim 0.07$, $\chi(T)$ is rapidly suppressed with decreasing temperatures. Here, the ground state of the system is spin singlet without degeneracy.

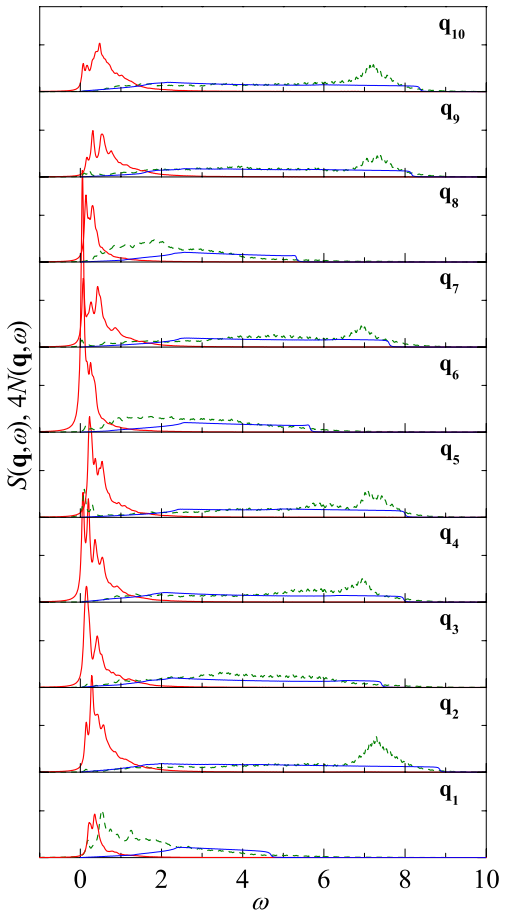

FIG. 5. (Color online) Calculated spin (solid line) and density (dashed line) excitation spectra of the t-J-K model at $J=-0.3$ and $K=0.06$. $\eta=0.04$ is assumed. We use the 20-site cluster with two vacancies ($n=0.9$). The spectra for the noninteracting infinite system $N_0(\mathbf{q},\omega)$ are also shown for comparison (thin solid line).

It should be noted that these results come basically from the finite-size effects of small clusters. However, we may infer the intrinsic nature of the infinite-size system and its K dependence from the low-energy behavior under the magnetic field. The results for $\chi(T)$ thus obtained are compared with experiment in Sec. IV.

D. Spin and density excitation spectra

The calculated results for the spin and density excitation spectra at $K=0.06$ are shown in Fig. 5. The excitation spectra for the corresponding noninteracting infinite-size system $N_0(\mathbf{q},\omega)=2S_0(\mathbf{q},\omega)$ are also shown for comparison. We find the following. The spectral weight for the spin excitations is concentrated on a very low-energy region of around $\omega \lesssim 1$. This reflects the presence of a large number of nearly degenerate low-energy states coming from the frustrated nature of the spin degrees of freedom. The low-energy spectral weight is extended over the entire Brillouin zone rather than special momenta, reflecting the spatially localized nature of the spin fluctuations. The spectral weight for the density excitations,

on the other hand, extends over a wide energy range of about $0<\omega\lesssim 9$ (entire bandwidth), which more or less resembles the spectrum of the noninteracting system.

From these results, we may say that the spin and density excitations are clearly separated in their energy scales: i.e., the spin excitations concentrate on the low-energy regions, the width of which scales with the exchange interactions (a combination of J and K), and the charge excitations extend over the entire bandwidth, which scales with the hopping parameter t of the vacancy. With increasing K, we find the upward shift of the low-energy spectral weight of the spin excitations; e.g., at $K=0.15-0.2$, we find the peaks at a higher-energy region of around $0<\omega\lesssim 5$, where the momentum dependence of the positions of the peaks becomes significant as well. Thus, the separation between the energy scales of the spin and density excitations becomes weaker. We also note that at $K=0$ where the ground state is fully spin polarized, the calculated spectra are quite different from those shown in Fig. 5.

We should note that the energy range where the spectral weight of the spin excitations accumulates (see Fig. 5), i.e., $0<\omega\lesssim 0.1$, corresponds well to the temperature range where the low-temperature sharp peak in the calculated specific heat $C(T)$ appears. We should also note that the broad spectra extending over the entire bandwidth correspond well to the very broad high-temperature peak in the calculated result for $C(T)$. We may therefore conclude that the separation between the spin and density excitations in their energy scales is responsible for the double-peak structure of the temperature dependence of the specific heat.

E. Single-particle excitation spectra

The calculated results for the single-particle excitation spectra $A(\mathbf{q},\omega)$ are shown in Fig. 6. From the results, we can deduce the possible quasiparticle band structure and hence the Fermi-surface topology. We find the following. There are broad and incoherent spectral features over a wide energy range corresponding to the total bandwidth of the noninteracting dispersion, i.e., $-5\lesssim\omega\lesssim 5$, but there emerge the sharp quasiparticlelike peaks with a characteristic dispersion in the vicinity of the Fermi energy. This result is similar to the case of the square-lattice t-J model near half filling.[18,19] Let us assume this to be the consequence of the presence of fermionic quasiparticles. Then, we find the quasiparticle band structure to be fitted well by the noninteracting band dispersion with a reduced hopping parameter t_{eff} or with an enhanced effective mass m^* of the quasiparticle (see Fig. 7). From the fitting, we find the value

$$t_{\mathrm{eff}}=\frac{m}{m^*}t\simeq(1/6)t \tag{9}$$

or $m^*/m\simeq 6$ at $n=0.9$ and $K=0.06$. The present results also suggest that the Fermi-surface topology of the quasiparticles is equivalent to that of the noninteracting system since the quasiparticle band can be obtained only by assuming that the bandwidth is reduced (or the band mass is enhanced). Thus, the Fermi surface is large (i.e., its area $\propto n$) rather than small [i.e., its area $\propto(1-n)$]. The doping dependence of m^* should

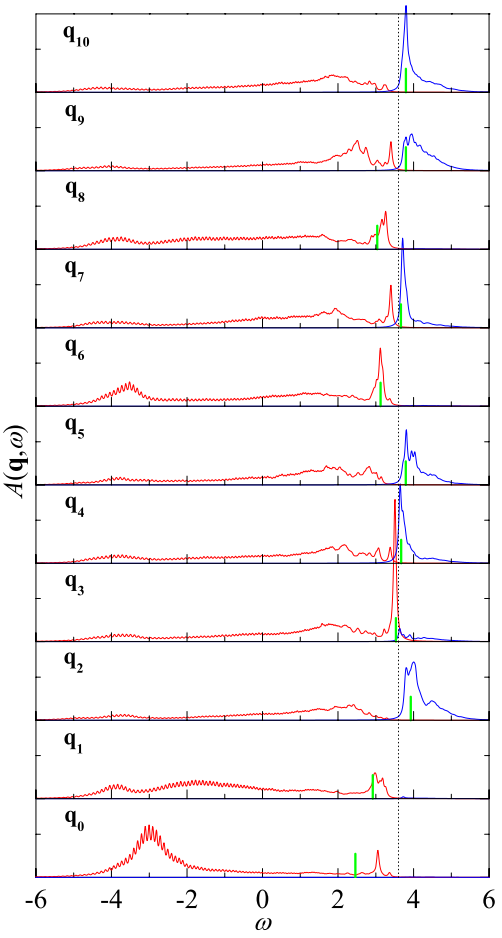

FIG. 6. (Color online) Calculated single-particle excitation spectra of the t-J-K model for the ground state of the 20-site cluster with two vacancies ($n=0.9$). Vertical dotted line represents the Fermi energy. Vertical bars represent the position of the noninteracting band dispersion with a reduced hopping parameter $t_{\mathrm{eff}}=t/6$. We assume $J=-0.3$, $K=0.06$, and $\eta=0.04$.

be interesting, in particular, whether m^* diverges or not at $n\rightarrow 1$. However, we cannot answer this question in our small-cluster study; the behavior of m^* even in the square-lattice t-J model still remains to be a puzzle.

We may also assume that the quasiparticle bandwidth shown in Fig. 7 may scale well with the energy of the spin excitations, i.e., a combination of the exchange parameters J and K, while the entire bandwidth ($\sim 9t$) of the broad spectral features shown in Fig. 6 scales with t, as in the case of the square-lattice t-J model near half filling.[18,19] Thus, we again find the separation between the spin and density degrees of freedom in their energy scales. The quasiholes (or quasiparticles as their conjugate) are thus the vacancies dressed by the spin excitations. We should note therefore that the spin and density degrees of freedom are not exactly separated in this sense, unlike in the Tomonaga-Luttinger liquid in the one-dimensional interacting fermion systems.[20] Only the energy scales are different. Further experimental and theoretical studies will be required to clarify the true low-energy physics of the system.

We may also point out that the enhanced effective mass of the quasiparticle band structure may partly be responsible for

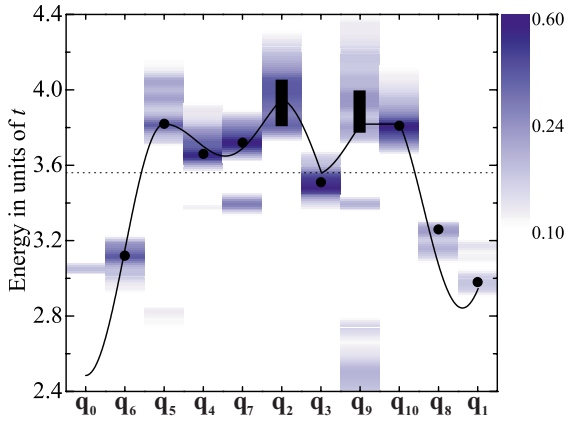

FIG. 7. (Color online) Quasiparticle band structure of the t-J-K model. Darkness of the shadow is in proportion to the spectral weight $A(\mathbf{q},\omega)$ shown in Fig. 6. Solid circles and bars represent the peak positions of the single-particle spectra. The peak positions are fitted with the noninteracting band structure (solid line) with a reduced hopping parameter $t_{\mathrm{eff}}=t/6$. Horizontal line is the Fermi energy.

the enhancement of the effective mass m^*/m determined from the specific-heat coefficient γ, although the latter cannot be obtained from our finite-size calculations. In Sec. IV, we compare the effective mass obtained from the quasiparticle band dispersion with experiment.

IV. COMPARISON WITH EXPERIMENT

The calculated results for the heat capacity $C(T)$ at $J=-0.3$ and $K=0.06$ (see Sec. III B) at the fillings of $n=0.92$ and 0.83 are compared with experiment in Fig. 8(a). We here assume the value of t determined so as to reproduce the higher-temperature peak observed in $C(T)$ at $n=0.92$, i.e., $t=43.8$ mK, so that we have $|J|=13.1$ mK and $K=2.63$ mK with keeping the ratio $t:|J|:K=1:0.3:0.06$. We also assume that the total area of the sample used in experiment (556 m^2) is uniformly active and contributes to the heat capacity. We should note that the results for the temperature region $T\lesssim 1$ mK are not reliable because of the finite-size effects where the discreteness of the energies in the system gives the exponential decay of the heat capacity at low temperatures.

We then find the fair agreement with experiment; in particular, the double-peak structure in $C(T)$, i.e., the lower-temperature peak that comes from the spin excitations and higher-energy peak that comes from the density excitations of the system, are reasonably well reproduced. More precisely, we find that our calculated results reproduce the experimental tendency that—near half filling—the lower-temperature peak is high, but with increasing the vacancy concentration, the higher-temperature peak becomes larger and simultaneously the peaks shift to higher temperatures.

Note that the specific-heat coefficient γ (or the effective mass) cannot be estimated from the present calculations of $C(T)$ due to finite-size effects. However, we find that the value of the enhanced effective mass $m^*/m\simeq 6$ estimated from the calculated quasiparticle band structure (see Sec. III E) is consistent with the experimental value $\sim 7.5-10$ estimated from the observed temperature dependence of $C(T)$ at $n=0.89$.[12] Here, we should note that the definition of m^* in the experimental specific-heat coefficient is twofold: one is the value deduced from the lower-temperature peak[21] and the other is the value deduced from the higher-temperature peak.[12] The two values are, however, not very different at least for $n\lesssim 0.9$, so that we can make comparison with our theoretical value. Then, it seems reasonable to assume that the renormalization of the band structure due to the spin excitations is mainly responsible for the observed enhancement of the effective mass.[12] Thus, stated differently, the specific-heat coefficient γ should be determined predominantly by the spin excitations of the system.

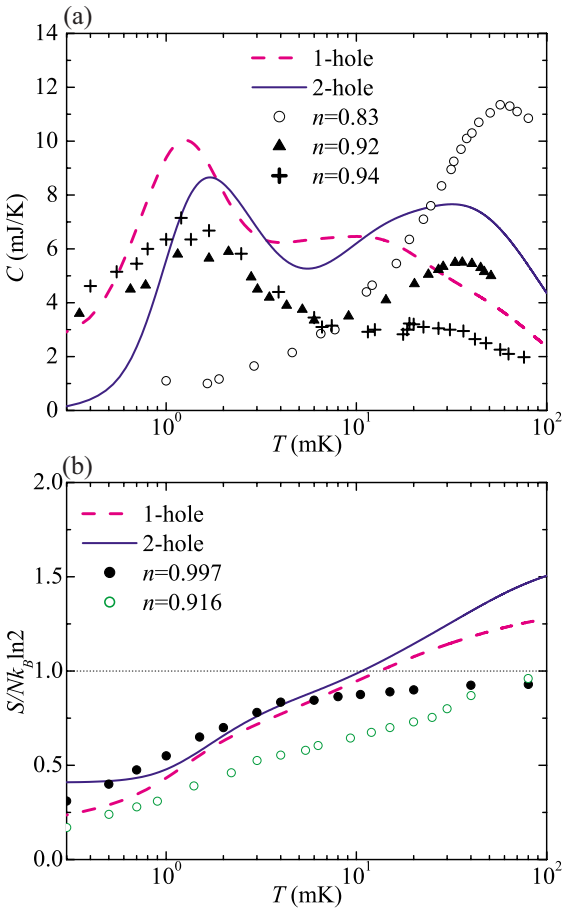

FIG. 8. (Color online) Temperature dependence of (a) the heat capacity $C(T)$ in units of mJ/K and (b) entropy $S(T)$ divided by the entropy of N free spins $Nk_B \ln 2$. Comparisons between theory (solid and dashed lines) and experiment (symbols) are shown. Experimental data are taken from Refs. 11 and 12.

The calculated results for the entropy $S(T)$ are also compared with experimentally determined[12] entropy in Fig. 8(b). We again find the fair agreement in their general tendencies. More precisely, we find that the calculated curves of $C(T)$ cross the line of the entropy of N free spins $Nk_B \ln 2$ at ~ 10 mK, at which the lower-temperature peak in $C(T)$ terminates. This result also supports that the lower-temperature peak in $C(T)$ comes from the excitations of the spin degrees of freedom of the system. The higher-energy peak should

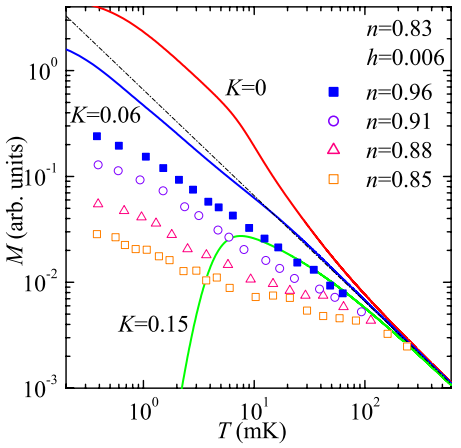

FIG. 9. (Color online) Temperature dependence of the magnetization M under the uniform magnetic field h. Comparison between theory (solid lines) and experiment (symbols) is shown. The straight line corresponds to the Curie law. Experimental data are taken from Ref. 23.

therefore come from the density degrees of freedom or motions of vacancies in the system. Note that the experimentally determined[12] entropy is significantly smaller than $Nk_B \ln 2$ even in the vicinity of half filling $n=0.997$ and even at temperatures of 10–20 mK where the lower-temperature peak in $C(T)$ terminates. The missing entropy may reside in the region of much lower temperatures that the present experiment does not approach.[22]

The calculated results for the magnetization under the uniform magnetic field are compared with experiment[23] in Fig. 9. We should note that the experimentally applied magnetic field ($\sim$170 mT), which is $h=0.006$ in our calculations, is very small in comparison with the energy scales of the ^{3}He system, so that the behavior of the magnetization under the uniform magnetic field is the same as that of the uniform magnetic susceptibility defined at $h \to 0$.

We find that although the finite-size effect is strong at low temperatures, the calculated magnetization at $K=0.06$ is consistent with experiment in the sense that the value is somewhat smaller than the value expected from the Curie law $M(T)=\chi(T)h=Ch/T$. For more quantitative comparison, however, one would need the techniques appropriate for treating infinite-size systems, so that experimentally observed plateaulike behavior[23] in the temperature dependence of the magnetization can be explained.

V. SUMMARY

We have used an exact-diagonalization technique on small clusters to study the low-energy physics of the triangular-lattice t-J model with the multiple-spin exchange interactions, whereby we have considered the anomalous properties observed in the doped Mott region of the two-dimensional liquid ^{3}He adsorbed on a graphite surface. We have calculated the temperature dependence of the specific heat, entropy, and uniform magnetic susceptibility, as well as the spin and density excitation spectra and single-particle spectra for the model, and have considered their implications.

We have shown the following. (1) The double-peak structure appears in the temperature dependence of the specific heat. The result is qualitatively consistent with experiment. The low-temperature sharp peak comes from the spin excitations and high-temperature broad peak comes from the density excitations. (2) The spectral weight for the spin excitations is concentrated on a very low-energy region, the width of which scales with the exchange interactions, while that of the density excitations extends over an entire bandwidth, which scales with the hopping parameter of the vacancy. The clear separation between spin and density excitations in their energy scales is thus found. (3) The accumulation of the spectral weight of the spin excitations comes from the frustrated nature of the spin degrees of freedom of the system; i.e., the ferromagnetic two-spin interactions J compete with the antiferromagnetic four-spin interactions K on the geometrically frustrated triangular lattice. (4) The single-particle excitation spectra suggest that the vacancies behave like the fermionic quasiparticles dressed by the spin excitations, of which the effective band mass is estimated to be $m^*/m \simeq 6$ at $n=0.9$, in consistent with the effective mass measured from the specific-heat coefficient. (5) The temperature dependence of the spin susceptibility shows a suppressed Curie-type behavior, reflecting the situation where the ground state is highly degenerate due to the frustrated nature of the spin degrees of freedom.

We hope that the present study will shed more light on the physics of the two-dimensional ^{3}He systems and stimulate further experimental and theoretical studies of the systems in greater details. We have focused on the doped Mott region of the monolayer ^{3}He in this paper. However, it has recently been reported[24] that the bilayer ^{3}He systems also contain rich physics concerning heavy fermions with quantum criticality, which we want to leave for future study.

ACKNOWLEDGMENTS

Enlightening discussions with Hiroshi Fukuyama and John Saunders are gratefully acknowledged. This work was supported in part by Grants-in-Aid for Scientific Research (Grants No. 18028008, No. 18043006, No. 18540338, and No. 19014004) from the Ministry of Education, Culture, Sports, Science and Technology of Japan. T.S. acknowledges financial support from JSPS Research Foundation for Young Scientists. A part of computations was carried out at the Research Center for Computational Science, Okazaki Research Facilities, and the Institute for Solid State Physics, University of Tokyo.

[1] For a recent review, see H. Fukuyama, J. Phys. Soc. Jpn. **77**, 111013 (2008), also see references therein.
[2] M. Roger, Phys. Rev. Lett. **64**, 297 (1990).
[3] M. Roger, C. Bäuerle, Yu. M. Bunkov, A.-S. Chen, and H. Godfrin, Phys. Rev. Lett. **80**, 1308 (1998).
[4] G. Misguich, B. Bernu, C. Lhuillier, and C. Waldtmann, Phys. Rev. Lett. **81**, 1098 (1998).
[5] T. Momoi, H. Sakamoto, and K. Kubo, Phys. Rev. B **59**, 9491 (1999).
[6] T. Momoi, P. Sindzingre, and N. Shannon, Phys. Rev. Lett. **97**, 257204 (2006).
[7] C. Bäuerle, Y. M. Bunkov, A. S. Chen, D. J. Cousins, H. Godfrin, M. Roger, and S. Triqueneaux, Physica B **280**, 95 (2000).
[8] S. Watanabe and M. Imada, J. Phys. Soc. Jpn. **76**, 113603 (2007).
[9] A. F. Andreev and I. M. Lifshitz, Sov. Phys. JETP **29**, 1107 (1969).
[10] H. Matsuda and T. Tsuneto, Prog. Theor. Phys. **46**, 411 (1970).
[11] Y. Matsumoto, D. Tsuji, S. Murakawa, H. Akisato, H. Kambara, and H. Fukuyama, J. Low Temp. Phys. **138**, 271 (2005).
[12] Y. Matsumoto, D. Tsuji, S. Murakawa, C. Bäuerle, H. Kambara, and H. Fukuyama (unpublished).
[13] Y. Fuseya and M. Ogata, J. Phys. Soc. Jpn. **78**, 013601 (2009).
[14] K. Seki, T. Shirakawa, and Y. Ohta, J. Phys.: Conf. Ser. (to be published).
[15] N. Shannon, B. Schmidt, K. Penc, and P. Thalmeier, Eur. Phys. J. B **38**, 599 (2004).
[16] N. Elstner and A. P. Young, Phys. Rev. B **50**, 6871 (1994).
[17] Y. Ohta, T. Nakaegawa, and S. Ejima, Phys. Rev. B **73**, 045101 (2006).
[18] R. Eder and Y. Ohta, Phys. Rev. B **50**, 10043 (1994).
[19] R. Eder, Y. Ohta, and S. Maekawa, Phys. Rev. Lett. **74**, 5124 (1995).
[20] See, e.g., T. Giamarchi, *Quantum Physics in One Dimension* (Oxford University Press, New York, 2004).
[21] A. Casey, H. Patel, J. Nyéki, B. P. Cowan, and J. Saunders, Phys. Rev. Lett. **90**, 115301 (2003).
[22] H. Fukuyama (private communication).
[23] S. Murakawa, H. Akisato, Y. Matsumoto, D. Tsuji, K. Mukai, H. Kambara, and H. Fukuyama, in *Low Temperature Physics: 24th International Conference on Low Temperature Physics - LT24*, AIP Conf. Proc. No. 850 (AIP, Melville, NY, 2006), p. 311.
[24] M. Neumann, J. Nyéki, B. Cowan, and J. Saunders, Science **317**, 1356 (2007).